In-Situ Component-Based TPA for Time-Variant Dynamic Systems: A State-Space Formulation

R. S. O. Dias[1], M. Martarelli[1], and P. Chiariotti[2]

[1]Department of Industrial Engineering and Mathematical Sciences
Università Politecnica delle Marche, Via Brecce Bianche, Ancona, 60131, Marche, Italy

[2]Department of Mechanical Engineering
Politecnico di Milano, Via Privata Giuseppe La Masa, Milan, 20156, Lombardia, Italy

ABSTRACT
In this article, a methodology to calculate equivalent forces by taking into account possible time-varying dynamic behaviour of the components under analysis is presented. This methodology is based on the use of the state-space realization of the in-situ component-based TPA method. To take into account possible time-varying dynamic behaviour of the systems under study, a local Linear Parameter Varying (LPV) model identification approach is used. This approach enables the computation of state-space models representative of the components at each time instant by interpolating a given set of Linear Time-Invariant (LTI) state-space models representative of the dynamics of the components under study for fixed operating conditions. By exploiting a numerical example, it is found that when dealing with structures presenting time-varying behaviour, accurate equivalent forces can be computed in time-domain by using the approaches presented in this paper. Furthermore, it is clearly demonstrated that ignoring the time dependency of the dynamic behaviour of mechanical systems can lead to an important deterioration of the results.

Keywords: Transfer Path Analysis, State-Space Substructuring, Linear Parameter-Varying (LPV) systems, System identification, State-Space Models

INTRODUCTION

Transfer Path Analysis (TPA) is a well-established technique in the Noise, Vibration and Harshness (NVH) field. During the last years, TPA has been exploited to study the transmission paths of noise and vibration from active components (i.e. sources) to the connected passive components (see, for example [1], [2], [3]). As the automotive field is concerned, it should be reported that the current TPA applications mainly exploit the frequency domain formulation. However, applications involving transient phenomena, such as ride comfort analysis while driving over bumps and the characterization of injector noise, would definitely benefit from the use of a TPA time-domain formulation. This paper points to those TPA applications targeted to the identification of loads in NVH (see, [4]). Namely, the family of component-based TPA methods, whose aim is the characterization of sources by a set of forces (also known as equivalent forces) that are an inherent property of the source itself. Several methods enabling time-domain force reconstruction are available in literature, for example based on adaptive algorithms [5] and on state-space models [6], [7]. However, less attention has been given to the time-domain computation of equivalent forces by taking into account possible time-variations on the dynamic behaviour of the components under study. Nevertheless, many mechanical systems are made of components that might present important dynamic time-dependent variations under operating conditions. A well-known example is represented by rubber mounts, whose mechanical behaviour depends on several parameters, like pre-load applied and temperature (see, [8]).

To take into account time-variations on the dynamics of the components under analysis, while computing equivalent forces, we aim at introducing a methodology based on the use of the state-space formulation. The benefit of using state-space models to deal with this kind of applications is justified by three main reasons. Firstly, the state-space models have an intrinsic suitability to deal with problems posed in time-domain, hence approaching these problems is easier by exploiting the state-space formulation. Secondly, by using this kind of models, the performance of time-domain simulations, which take into account variations on the dynamic behaviour of the components under study, is simplified. Thirdly, it is widely known that the state-space formulation is one of the best choices for real-time applications.

The methodology here presented is based on the use of the state-space realization of the in-situ component-based TPA method. To account for time-variations on the dynamic behaviour of the components under analysis we propose the use of local Linear Parameter-Varying (LPV) model identification approaches (see [9], [10], [11]). These approaches enable the interpolation of Linear time-invariant (LTI) state-space models representative of the dynamics of the components under study for constant values of the scheduling parameters, i.e. for fixed operating conditions. Thereby, it becomes possible to estimate state-space models representative of the operating conditions of the target component at each time sample, without the need to experimentally characterize the component for each individual operating condition.

The state-space realization of the in-situ component-based TPA method is presented in section "In-Situ Component-Based TPA". Then, guidelines on how to implement a local LPV model identification approach are provided in section "Linear Parameter-Varying models". In section "Numerical Example", the approaches discussed in this paper are validated by using a numerical example. Finally, in section "Conclusion" the conclusion is presented.

IN-SITU COMPONENT-BASED TPA

In this section, the in-situ method of the component-based TPA family (see [4]) will be extended into the state-space domain. It is worth mentioning that the state-space realization of this method will be presented by assuming an estimation of the forces in a linear least-squares sense (perhaps, the most straightforward way to compute the intended forces). Nevertheless, it is well-known from literature that the force identification problem is ill-posed. Moreover, in an experimental scenario, estimating forces in a linear least-squares sense does not lead in general to useful results, as it generally amplifies the noise in the used operational outputs to estimate the forces (see, for instance [12], [7]). More robust methodologies to solve the force identification problem are available in literature (see, for instance [6], [7], [13]). However, these approaches will not be here investigated, because the sole aim of this paper is to theoretically introduce a methodology to account for time-variations on the dynamic behaviour of components when calculating equivalent forces. For this reason, a discussion on the most suitable methods to estimate time-domain forces is out of the scope of this article.

To start approaching the in-situ component-based TPA method, let us consider the assembled structure of figure 1, where a source and a passive component are connected together. By using component-based TPA methods, we aim at characterizing the source by a set of forces that are an inherent property of the source itself. These forces are commonly tagged as equivalent forces and, when applied on the active component A at rest, the operational responses (i.e when the source is turned on) at the passive component can be simulated (see figure 1b). Moreover, as the equivalent forces are only a property of the source, they can be used to determine the operational responses at any passive system connected with the source [4], [14].

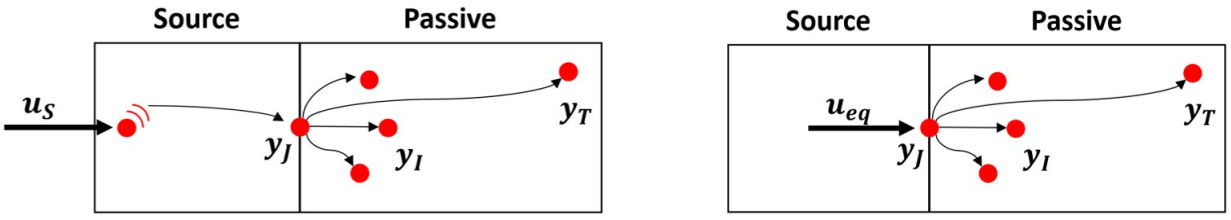

(a) Operational responses originated by the internal forces generated by the internal mechanisms of the source.

(b) Operational responses originated by the equivalent forces determined with component-based TPA.

Figure 1: Assembled structure composed by a source and a passive substructure.

At this point, we may compute the operational acceleration responses at the indicators location of the structure given in figure 1, by either using the internal forces generated by the internal mechanisms of the source or by applying the set of equivalent

forces at the interface between the source and the passive system. By computing those operational responses by following both mentioned approaches, we obtain the following identity

$$[\bar{H}_{TJ}(j\omega)]\left\{U_{J,eq}(j\omega)\right\} = [\bar{H}_{TS}(j\omega)]\left\{U_S(j\omega)\right\} \tag{1}$$

where, $\left\{U_{J,eq}(j\omega)\right\} \in \mathbb{C}^{n_J \times 1}$ is the vector of equivalent forces in frequency domain, $[H(j\omega)] \in \mathbb{C}^{n_o \times n_i}$ denotes an acceleration FRF matrix and overbar variables denote variables associated with the assembled structure. Variables n_i and n_o represent the number of inputs and outputs, respectively, whereas n_J represents the number of interface DOFs. Subscript S and J denote variables associated with internal DOFs belonging to the source and with the interface DOFs, respectively, while subscripts I and T denote variables associated with indicators and targets DOFs, respectively (see figure 1). From expression (1) we may establish a relation between the internal forces generated on the source and the set of equivalent forces as given below.

$$\left\{U_{J,eq}(j\omega)\right\} = [\bar{H}_{TJ}(j\omega)]^{-1}[\bar{H}_{TS}(j\omega)]\left\{U_S(j\omega)\right\} \tag{2}$$

It can be proven that the following relation holds (see [4])

$$[\bar{H}_{TJ}(j\omega)]^{-1}[\bar{H}_{TS}(j\omega)] = \left[H^S_{JJ}(j\omega)\right]^{-1}\left[H^S_{JS}(j\omega)\right] \tag{3}$$

where, superscript S denotes variables associated with the source. Expression (2) can be rewritten as follows

$$\left\{U_{J,eq}(j\omega)\right\} = \left[H^S_{JJ}(j\omega)\right]^{-1}\left[H^S_{JS}(j\omega)\right]\left\{U_S(j\omega)\right\} \tag{4}$$

or, by using state-space matrices

$$\left\{U_{J,eq}(j\omega)\right\} = \left(\left[C^S_{J,accel}\right](j\omega[I] - \left[A^S\right])^{-1}\left[B^S_J\right] + \left[D^S_{JJ,accel}\right]\right)^{-1}\left(\left[C^S_{J,accel}\right](j\omega[I] - \left[A^S\right])^{-1}\left[B^S_S\right] + \left[D^S_{JS,accel}\right]\right)\left\{U_S(j\omega)\right\} \tag{5}$$

where, subscript *accel* denotes matrices of an acceleration state-space model (state-space model, whose output vector elements are accelerations). Expressions (4) and (5) prove that the equivalent forces are a property of the source. The set of equivalent forces may also be computed in time-domain. It is worth mentioning that as we are using state-space models possible changes on the dynamic properties of both source and passive components over time can be taken into account to compute the equivalent forces. Hence in the following, when working in the time-domain, the state-space matrices will be assumed to be time dependent. In this way, we may calculate the equivalent forces in time-domain as follows

$$\begin{aligned}\left\{\dot{x}^{S,inv}(t)\right\} &= \left[A^{S,inv}(t)\right]\left\{x^{S,inv}(t)\right\} + \left[B^{S,inv}_J(t)\right]\left\{\ddot{y}^S_J(t)\right\}\\ \left\{u_{J,eq}(t)\right\} &= \left[C^{S,inv}_J(t)\right]\left\{x^{S,inv}(t)\right\} + \left[D^{S,inv}_{JJ}(t)\right]\left\{\ddot{y}^S_J(t)\right\}\end{aligned} \tag{6}$$

where, $\{x(t)\} \in \mathbb{R}^{n\times 1}$ is the state vector, $\{u(t)\} \in \mathbb{R}^{n_i \times 1}$ is the input vector. Variable n represents the number of states, matrices $[A^{S,inv}(t)]$, $[B^{S,inv}(t)]$, $[C^{S,inv}(t)]$ and $[D^{S,inv}(t)]$ are given as follows

$$\begin{aligned}[A^{S,inv}(t)] = [A^S(t)] - [B^S_J(t)][D^S_{JJ,accel}(t)]^{-1}[C^S_{J,accel}(t)], \quad [B^{S,inv}_J(t)] = [B^S_J(t)][D^S_{JJ,accel}(t)]^{-1}\\ [C^{S,inv}_J(t)] = -[D^S_{JJ,accel}(t)]^{-1}[C^S_{J,accel}(t)], \quad [D^{S,inv}_{JJ}(t)] = [D^S_{JJ,accel}(t)]^{-1}\end{aligned} \tag{7}$$

while, the acceleration responses $\{\ddot{y}^S_J(t)\}$ must be computed by exploiting the state-space model given below.

$$\begin{aligned}\{\dot{x}^S(t)\} &= \left[A^S(t)\right]\{x^S(t)\} + \left[B_S^S(t)\right]\{u_S(t)\} \\ \left\{\ddot{y}_J^S(t)\right\} &= \left[C_{J,accel}^S(t)\right]\{x^S(t)\} + \left[D_{JS,accel}^S(t)\right]\{u_S(t)\}\end{aligned} \tag{8}$$

Even though by using expression (5) it is possible to compute the set of equivalent forces, we are required to know the internal forces caused by the internal mechanism of the source. In practice, these forces are generally impossible to measure. To circumvent this requirement, we may calculate the set of equivalent forces by following the in-situ method proposed by Moorhouse and Elliott (see [15], [16]). This method holds the advantage of avoiding the use of special test-rigs and the need of dismounting any component. By exploiting this approach we may calculate the equivalent forces at the interface of the assembly given in figure 1 as follows

$$\left\{U_{J,eq}(j\omega)\right\} = \begin{bmatrix}\bar{H}_{JJ}(j\omega)\\ \bar{H}_{IJ}(j\omega)\\ \bar{H}_{TJ}(j\omega)\end{bmatrix}^{\dagger}\begin{Bmatrix}\ddot{\bar{Y}}_J(j\omega)\\ \ddot{\bar{Y}}_I(j\omega)\\ \ddot{\bar{Y}}_T(j\omega)\end{Bmatrix} \tag{9}$$

where, superscript † denotes the Moore-Penrose pseudoinverse of a matrix. By using state-space matrices, expression (9) can be rewritten as given below.

$$\left\{U_{J,eq}(j\omega)\right\} = \begin{bmatrix}[\bar{C}_{J,accel}](j\omega[I]-[\bar{A}])^{-1}[\bar{B}_J]+[\bar{D}_{JJ,accel}]\\ [\bar{C}_{I,accel}](j\omega[I]-[\bar{A}])^{-1}[\bar{B}_J]+[\bar{D}_{IJ,accel}]\\ [\bar{C}_{T,accel}](j\omega[I]-[\bar{A}])^{-1}[\bar{B}_J]+[\bar{D}_{TJ,accel}]\end{bmatrix}^{\dagger}\begin{Bmatrix}\ddot{\bar{Y}}_J(j\omega)\\ \ddot{\bar{Y}}_I(j\omega)\\ \ddot{\bar{Y}}_T(j\omega)\end{Bmatrix} \tag{10}$$

The equivalent forces can also be computed in time-domain by using the in-situ method as follows

$$\begin{aligned}\{\dot{x}(t)\} &= \left[\bar{A}^{inv}(t)\right]\{x(t)\} + \left[\bar{B}_J^{inv}(t)\right]\begin{Bmatrix}\ddot{\bar{y}}_J(t)\\ \ddot{\bar{y}}_I(t)\\ \ddot{\bar{y}}_T(t)\end{Bmatrix} \\ \left\{u_{J,eq}(t)\right\} &= \left[\bar{C}_{JIT}^{inv}(t)\right]\{x(t)\} + \left[\bar{D}_{JIT,J}^{inv}(t)\right]\begin{Bmatrix}\ddot{\bar{y}}_J(t)\\ \ddot{\bar{y}}_I(t)\\ \ddot{\bar{y}}_T(t)\end{Bmatrix}\end{aligned} \tag{11}$$

where,

$$\begin{aligned}[\bar{A}^{inv}(t)] &= [\bar{A}(t)] - [\bar{B}_J(t)][\bar{D}_{JIT,J}(t)]^{\dagger}[\bar{C}_{JIT}(t)], \quad [\bar{B}_J^{inv}(t)] = [\bar{B}_J(t)][\bar{D}_{JIT,J}(t)]^{\dagger} \\ [\bar{C}_{JIT}^{inv}(t)] &= -[\bar{D}_{JIT,J}(t)]^{\dagger}[\bar{C}_{JIT}(t)], \quad [\bar{D}_{JIT,J}^{inv}(t)] = [\bar{D}_{JIT,J}(t)]^{\dagger}\end{aligned} \tag{12}$$

matrices $[\bar{C}_{JIT}(t)]$ and $[\bar{D}_{JIT,J}(t)]$ are given below.

$$\left[\bar{C}_{JIT}(t)\right] = \begin{bmatrix}\bar{C}_{J,accel}(t)\\ \bar{C}_{I,accel}(t)\\ \bar{C}_{T,accel}(t)\end{bmatrix}, \quad [\bar{D}_{JIT,J}(t)] = \begin{bmatrix}\bar{D}_{JJ,accel}(t)\\ \bar{D}_{IJ,accel}(t)\\ \bar{D}_{TJ,accel}(t)\end{bmatrix} \tag{13}$$

Note that for the sake of completeness, in expressions (9), (10) and (11), we presented how to calculate the equivalent forces from measured operational responses at the interface, indicators and targets locations. Nevertheless, in practice the equivalent forces are solely determined from operational responses measured at the indicators (see [4]). In fact, the responses acquired at the target DOFs are usually not used, because they are many times small in number and placed far away from the interface. Consequently, they do not properly observe the interface between the source and the passive system. On the other hand, the

responses at the interface DOFs are usually difficult to measure as it requires the placement of sensors at the interface, which implies practical difficulties. Conversely, the location of the indicator DOFs is specially chosen to be accessible and close to the interface to properly observe it. Furthermore, the number of these DOFs is typically at least two times higher than the number of equivalent forces to be determined in order to guarantee over-determination and, hence better matrix conditioning [4].

Note also that, as proven above, the equivalent forces are a property of the source, hence the equivalent forces computed by using the in-situ method continue to be valid to simulate the operational responses at any passive component to which the source is coupled. However, to successfully compute the equivalent forces by exploiting the in-situ method, we must guarantee that the operational excitation only comes from the source and that the measured operational responses used to compute the equivalent forces are acquired at the passive component or at the interface between the source and the passive system [4].

LINEAR PARAMETER-VARYING MODELS

In this section, we will present how to estimate Linear Parameter-Varying models by using a local approach. The local approaches enable the interpolation of LTI state-space models representative of the dynamics of the component under study for constant values of the scheduling parameters, i.e. for fixed operating conditions, thus making the identification of the state-space model representations of the operating conditions of the target components possible, with no need to experimentally characterize the component for each individual operating condition. We will assume that the LTI state-space models used to construct the LPV model are displacement state-space models. The use of displacement models is indeed advantageous, because by definition these models present null feed-through matrices, thus the number of variables involved on the computation of the LPV model decreases. Consequently, the computational cost for computing the LPV models and the cost of computing the interpolated state-space models for each of the intermediate operational conditions also decreases.

To start, we must define the operating conditions for which a set of LTI models will be estimated. There are no strict rules on which operating conditions to choose. Nevertheless, for a system depending on a scheduling parameter β, whose value varies from a minimum value of $\underline{\beta}$ to a maximum value of $\bar{\beta}$, it is recommended that one of the chosen operating conditions be characterized by a β slightly lower or equal to $\underline{\beta}$; in addiction one of the chosen operating conditions must be characterized by a β equal or slightly higher than $\bar{\beta}$. In this way, we make sure that there is no need of performing extrapolation to characterize the dynamic behavior of the target component. It is also suggested to choose operating conditions characterized by an equidistant value of the scheduling parameter. Moreover, the number of used LTI models must be as small as possible (to reduce the number of state-space models to be identified), but large enough to well-capture the influence of the scheduling parameter over the target component dynamics [10].

To successfully compute a LPV model from a given set of LTI models, we must firstly transform the models into a coherent representation. When the set of state-space models is directly constructed from the mechanical properties of the component under analysis (in an analytical or numerical scenario), they are already obtained in a coherent representation. However, in an experimental context the state-space models are in general computed from experimentally acquired data by using system identification algorithms, for instance by using the well-known n4sid methods (see [17], [18]) or the procedures presented in [19], [20], which rely on a previous modal identification step by using PolyMAX [21] and ML-MM methods [22]. In this scenario, the estimated set of state-space models is generally not obtained in a coherent representation. In literature, several approaches to transform the estimated set of state-space models into a coherent representation have been proposed (for example, see [23], [11]). Here, to transform the set of estimated state-space models into a coherent representation, we will start by transforming each of the state-space models into modal form as follows

$$\begin{aligned} \{\dot{x}_{mf}(t)\} &= [A_{mf}]\{x_{mf}(t)\} + [B_{mf}]\{u_{mf}(t)\} \\ \{y_{mf}(t)\} &= [C_{mf}]\{x_{mf}(t)\} \end{aligned} \tag{14}$$

where, subscript mf denotes matrices/vectors associated with a state-space model transformed into modal form, whereas matrices $[A_{mf}]$, $[B_{mf}]$ and $[C_{mf}]$ are given in (15).

$$[A_{mf}] = [\Lambda] = [T_{mf}]^{-1}[A][T_{mf}], \quad [B_{mf}] = [T_{mf}]^{-1}[B], \quad [C_{mf}] = [C][T_{mf}] \tag{15}$$

In Eq. (15), $[\Lambda]$ is a diagonal matrix containing the eigenvalues of matrix $[A]$ (which are also the poles of the system) and $[T_{mf}]$

is a modal matrix containing all system eigenvectors as columns and can be computed by solving the eigenvalue problem given below.

$$[A][T_{mf}] = [T_{mf}][\Lambda]. \tag{16}$$

As next step, we must ensure that the poles of each state-space model of the set of identified models (which are present in the diagonal of the state matrices) are sorted in a coherent way. Each pole has an associated natural frequency and damping ratio, hence to take in account both values, we will sort the poles in ascending damped natural frequency. The damped natural frequency of a pole can be simply computed as follows

$$\omega_d^r = \omega_n^r \sqrt{1 - (\xi^r)^2} \tag{17}$$

where, ω_d^r and ω_n^r are the damped natural frequency and the natural frequency of the r^{th} pole, respectively, while ξ^r is the damping ratio of the r^{th} pole. Note that, eventual ties when sorting pairs of complex conjugate poles are broken by firstly including the pole presenting positive imaginary part and by including afterwards the pole presenting negative imaginary part. The rows of the input matrix and the columns of the output matrix must be sorted in accordance with the poles.

Then, we must coherently scale the matrices $[B_{mf}]$ and $[C_{mf}]$ of each state-space model of the estimated set of models. The need for scaling both input and output matrices arises because the modal domain representation of a state-space model is not unique with respect to these scalings. Thus, to ensure a smooth variation of the coefficients of both input and output matrices a coherent scaling is mandatory [23]. In this way, we may define the scaling of both input and output matrices as follows

$$[B_{mf,sc}] = [W]^{-1}[B_{mf}] \tag{18}$$

$$[C_{mf,sc}] = [C_{mf}][W] \tag{19}$$

where, subscript *sc* denotes a coherently scaled state-space matrix, while $[W] \in \mathbb{C}^{n \times n}$ is the scaling matrix. A straightforward approach to coherently scale all the estimated state-space models is, for instance, to normalize each row of the $[B_{mf}]$ matrix associated to each of the poles of the system with respect to one of its elements [23]. Assuming that a normalization with respect to the first element of each row of $[B_{mf}]$ is chosen, the $[W]$ matrix must be constructed as follows

$$[W] = \begin{bmatrix} B_{11,mf} & & \\ & B_{21,mf} & \\ & & \ddots \end{bmatrix} \tag{20}$$

where, the first and second subscripts denote the number of the row and column of the input matrix element, respectively. It is worth mentioning that by using the scaling matrix given in expression (20), the input-output properties of the state-space models are unchanged. To demonstrate this, we may compute the FRFs of the scaled state-space model as given below.

$$[H_{mf,sc}(j\omega)] = [C_{mf}][W](j\omega[I] - [\Lambda])^{-1}[W]^{-1}[B_{mf}] = [C_{mf}](j\omega[I] - [\Lambda])^{-1}[B_{mf}] \tag{21}$$

By observing expression (21) and having in mind that matrices $[W]$ and $[\Lambda]$ are diagonal matrices, we may conclude that by scaling state-space models with $[W]$ the FRFs of the state-space model are not changed and hence, the input-output properties of the model remain unchanged. The scaling approach just presented will be exploited in the numerical example discussed in section "Numerical Example".

After having represented the set of state-space models coherently, an LPV model can be constructed. To define the LPV model we will follow the procedure proposed by De Caigny et al. in [10]. This approach assumes that the interpolating LPV model

to be constructed presents a homogeneous polynomial dependency on the parameterized values that the scheduling parameters take in a multisimplex Λ.

Let us assume that by using an interpolating LPV model, we aim at estimating a state-space model representative of the dynamics of a structure for a fixed operating condition l that is characterized by a single scheduling parameter β. A parameterization of β in the multisimplex Λ of dimension $N = 2$ (common choice in practice [10]) can be defined as follows

$$\alpha_{l,1} = \frac{\beta_l - \underline{\beta}}{\bar{\beta} - \underline{\beta}}, \quad \alpha_{l,2} = 1 - \alpha_{l,1} \tag{22}$$

where, $\bar{\beta}$ and $\underline{\beta}$ are the maximum and minimum values of the scheduling parameter associated with the set of state-space models used to define the LPV model, respectively.

After having parameterized the scheduling parameter, we may define the interpolated state-space matrices representative of the fixed operating condition l by using a LPV model as follows

$$diag[A(\alpha_l)] = \sum_{k=1}^{J_N(g)} \alpha_l^k \{\tilde{A}^k\} \tag{23a}$$

$$[B(\alpha_l)] = \sum_{k=1}^{J_N(g)} \alpha_l^k [\tilde{B}^k] \tag{23b}$$

$$[C(\alpha_l)] = \sum_{k=1}^{J_N(g)} \alpha_l^k [\tilde{C}^k] \tag{23c}$$

where, $diag[\bullet]$ is a column vector containing the diagonal elements of matrix $[\bullet]$, α_l^k represents the element placed on the k^{th} column of $\{\alpha_l\}$, which assuming an homogeneous polynomial dependency of degree g must be computed as given below.

$$\{\alpha_l\} = \begin{bmatrix} \alpha_{l,1}^g \alpha_{l,2}^0 & \alpha_{l,1}^{g-1} \alpha_{l,2}^1 & \dots & \alpha_{l,1}^0 \alpha_{l,2}^g \end{bmatrix} \tag{24}$$

It is worth mentioning that all the coefficients of the vector $\{\alpha_l\}$ must present the same degree g, because by exploiting the approach proposed in [10], we assume that the LPV model to be set-up presents an homogeneous polynomial dependency on the parameterized values of the scheduling parameter. Moreover, $\{\alpha_l\}$ should be composed by a number of elements given by the expression presented below.

$$J_N(g) = \frac{(N+g-1)!}{g!(N-1)!} \tag{25}$$

The variables $\{\tilde{A}^k\} \in \mathbb{C}^{n \times 1}$, $[\tilde{B}^k] \in \mathbb{C}^{n \times n_i}$ and $[\tilde{C}^k] \in \mathbb{C}^{n_o \times n}$ in expression (23) are unknown vectors/matrices associated with the monomial positioned on the k^{th} column of $\{\alpha_l\}$. These variables must be determined in order to define the interpolating LPV model. A straightforward approach is determining those unknown vectors/matrices in a linear least-squares sense. In this way, we must define our problem as follows

$$[a]\{q\} = \{b\} \tag{26}$$

where,

$$[a] = \begin{bmatrix} \alpha_1 \bigotimes I_{A,A} & & & \\ \vdots & & & \\ \alpha_m \bigotimes I_{A,A} & & & \\ & \alpha_1 \bigotimes I_{B,B} & & \\ & \vdots & & \\ & \alpha_m \bigotimes I_{B,B} & & \\ & & \alpha_1 \bigotimes I_{C,C} & \\ & & \vdots & \\ & & \alpha_m \bigotimes I_{C,C} & \end{bmatrix} \tag{27a}$$

$$\{q\} = \left\{ \{\tilde{A}^1\}^T \quad \dots \quad \{\tilde{A}^{J_N(g)}\}^T \quad (vec[\tilde{B}^1])^T \quad \dots \quad (vec[\tilde{B}^{J_N(g)}])^T \quad (vec[\tilde{C}^1])^T \quad \dots \quad (vec[\tilde{C}^{J_N(g)}])^T \right\}^T \tag{27b}$$

$$\{b\} = \left\{ (diag[\Lambda^1])^T \quad \dots \quad (diag[\Lambda^m])^T \quad (vec[B^1_{mf,sc}])^T \quad \dots \quad (vec[B^m_{mf,sc}])^T \quad (vec[C^1_{mf,sc}])^T \quad \dots \quad (vec[C^m_{mf,sc}])^T \right\}^T \tag{27c}$$

where, $\bigotimes$ denotes the Kronecker matrix product, matrices $[I_{A,A}]$, $[I_{B,B}]$ and $[I_{C,C}]$ are identity matrices of dimension n, nn_i and nn_o, respectively, $vec[\bullet]$ is the vector obtained by stacking all columns of matrix $[\bullet]$ and m is the number of state-space models included in the set of estimated state-space models. Note that, as the state-space models used to construct the LPV model are transformed in modal form, their state matrix is a diagonal matrix. This is the reason why to construct the vector $\{b\}$, we only use the diagonal elements of the state matrices of each state-space model. Indeed, the construction of an LPV model by using state-space models transformed into modal form is interesting in the sense that the state matrix of each of the estimated LTI models becomes a diagonal matrix. Thus, to define the partition of the interpolating LPV model responsible for calculating the state matrices of the interpolated models, we are only required to determine unknown vectors composed by n elements instead of unknown matrices composed by n^2 elements.

At this point, to compute vector $\{q\}$ in a linear least-squares sense, we may use the following expression.

$$\{q\} = [a]^{\dagger}\{b\} \tag{28}$$

Obviously, by calculating the unknown parameters as presented above, we aim at minimizing the squared 2-norm of the errror vector given below.

$$[F(q)] = - \begin{bmatrix} \sum_{k=1}^{J_N(g)} \alpha_1^k \{\tilde{A}^k\} - diag[\Lambda^1] \\ \vdots \\ \sum_{k=1}^{J_N(g)} \alpha_m^k \{\tilde{A}^k\} - diag[\Lambda^m] \\ \sum_{k=1}^{J_N(g)} \alpha_1^k vec[\tilde{B}^k] - vec[B^1_{mf,sc}] \\ \vdots \\ \sum_{k=1}^{J_N(g)} \alpha_m^k vec[\tilde{B}^k] - vec[B^m_{mf,sc}] \\ \sum_{k=1}^{J_N(g)} \alpha_1^k vec[\tilde{C}^k] - vec[C^1_{mf,sc}] \\ \vdots \\ \sum_{k=1}^{J_N(g)} \alpha_m^k vec[\tilde{C}^k] - vec[C^m_{mf,sc}] \end{bmatrix} \tag{29}$$

NUMERICAL EXAMPLE

In this section, a numerical example will be studied to validate the approaches discussed in this paper. The numerical example to be analyzed involves three different components, from now on labelled as components A, B and C (see figure 2). Moreover, two assembled structures will be analyzed, one of the assemblies is originated from the coupling of components A and B (from now on tagged as assembly AB), while the other one is originated from the coupling of components A and C (from now on denoted as assembly AC). Both assemblies are depicted in figure 3, whereas the value of the physical parameters labelled in figures 2 and 3 is provided in table 1.

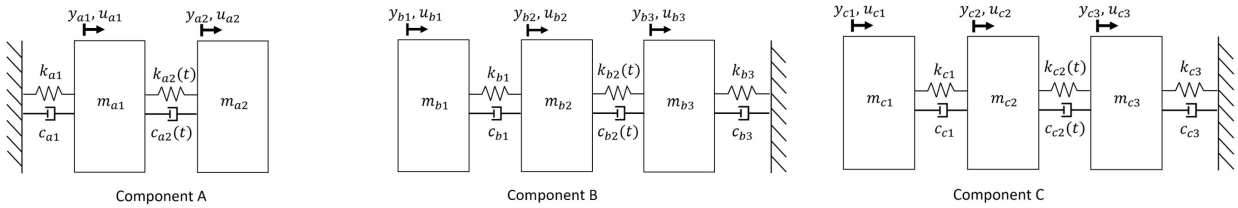

Figure 2: Components.

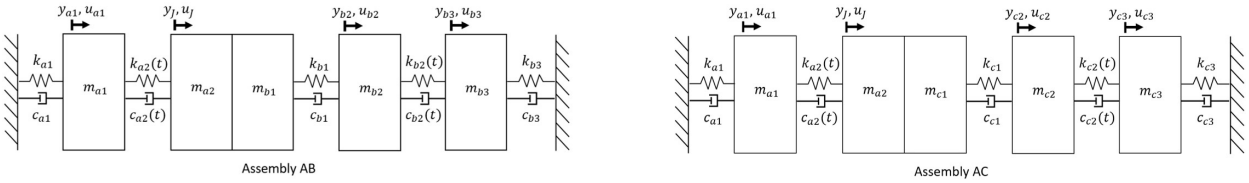

Figure 3: Assemblies.

Table 1: Physical parameter values

i	m_i (kg)	c_i (N s m^{-1})	k_i (N m^{-1})
$a1$	6	10	4×10^3
$a2$	4	$(5)^{n_1(t)}$	$(2 \times 10^3)^{n_1(t)}$
$b1$	5	20	1×10^3
$b2$	3	$(15)^{n_2(t)}$	$(3.5 \times 10^3)^{n_2(t)}$
$b3$	1.5	5	4×10^3
$c1$	7	10	5×10^3
$c2$	3.5	$(20)^{n_3(t)}$	$(7.5 \times 10^3)^{n_3(t)}$
$c3$	5	12	1×10^3

To start approaching the numerical example, analytical state-space models representative of the three components and of the two assemblies were directly defined from their correspondent mass, stiffness and damping matrices. For simplicity the damping matrix of each system was constructed from the stiffness one by replacing the stiffness terms by damping ones. Moreover, one stiffness and one damping parameter associated with components A, B and C present a non-linear variation with respect to the value of variables n_1, n_2 and n_3, respectively. The value of these variables is assumed to vary over time as depicted in figure 4. Each of the curves shown in this figure were discretized with a sampling frequency of 2×10^4 Hz. Then, for each mechanical system, analytical state-space models were computed at each time sample.

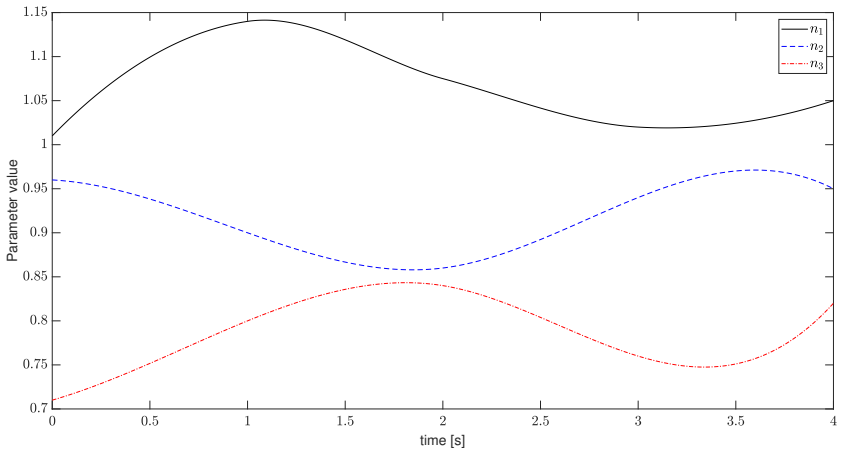

Figure 4: Variation of the value of parameters n_1, n_2 and n_3 over time.

After having computed the analytical state-space models, an LPV model for each of the three components must be defined. It was found that four different state-space models representative of the dynamics of each component for four different operating conditions is enough to capture the influence of parameters n_1, n_2 and n_3 on the dynamics of components A, B and C, respectively. The value of the time dependent parameters associated with the set of state-space models used to define each of the LPV models is shown in table 2. The state-space models used to define the LPV models representative of components A, B and C were obtained analytically and then were transformed into modal form (see expression (15)). In this way, the sets of state-space models used to construct each of the LPV models were not directly represented in a coherent form (which is the common situation in practice). Thus, the procedures discussed in section "Linear Parameter-Varying models" were applied to coherently represent each set of state-space models. To scale both output and input matrices of each state-space model, a normalization of each row of the input matrix with respect to the first input was performed. Figures 5, 6 and 7 show the comparison of some FRFs of the set of analytical state-space models with the FRFs of the correspondent coherent representation used to set-up the LPV models for components A, B and C, respectively. By observing these figures, we may verify that by scaling both output and input matrices as discussed in section "Linear Parameter-Varying models", the FRFs of the state-space models remain unchanged. Therefore, the input-output properties of the models are also not affected by the scaling procedure.

Table 2: Parameter values at the fixed operating conditions used to define the LPV models

Parameter	Fixed Condition 1	Fixed Condition 2	Fixed Condition 3	Fixed Condition 4
n_1	1	1.05	1.1	1.15
n_2	0.85	0.9	0.95	1
n_3	0.7	0.75	0.8	0.85

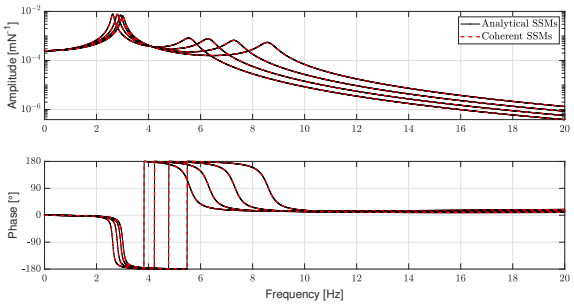

(a) Displacement FRFs, whose output is the DOF a_1 and the input is the DOF a_2.

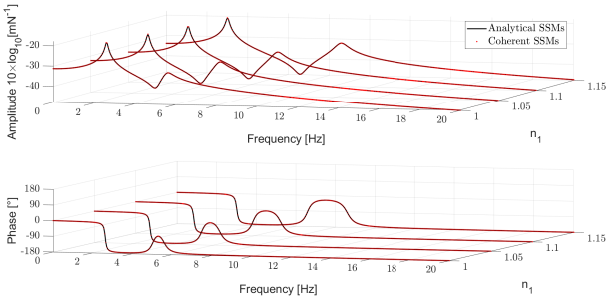

(b) Driving point displacement FRFs, whose output and input is the DOF a_2.

Figure 5: Comparison of some displacement FRFs of the set of analytical state-space models with the same displacement FRFs of their correspondent coherent representation used to set-up an LPV model representative of the dynamics of component A.

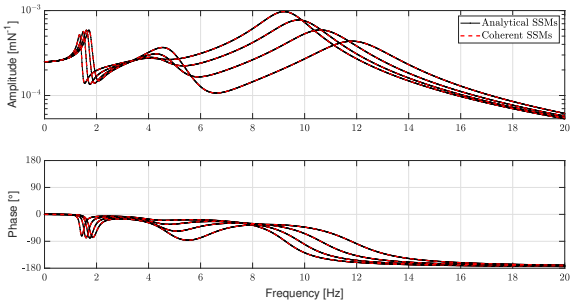

(a) Driving point displacement FRFs, whose output and input is the DOF b_3.

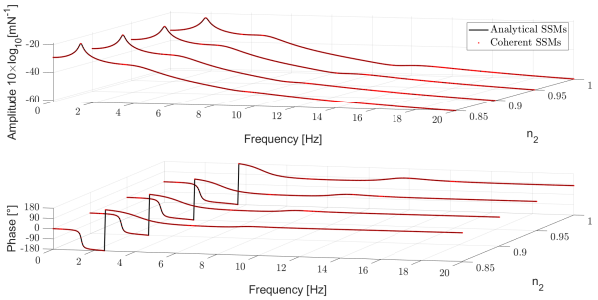

(b) Displacement FRFs, whose output is the DOF b_1 and the input is the DOF b_2.

Figure 6: Comparison of some displacement FRFs of the set of analytical state-space models with the same displacement FRFs of their correspondent coherent representation used to set-up an LPV model representative of the dynamics of component B.

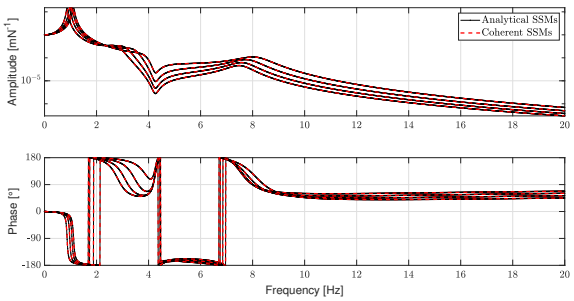

(a) Displacement FRFs, whose output is the DOF c_2 and the input is the DOF c_3.

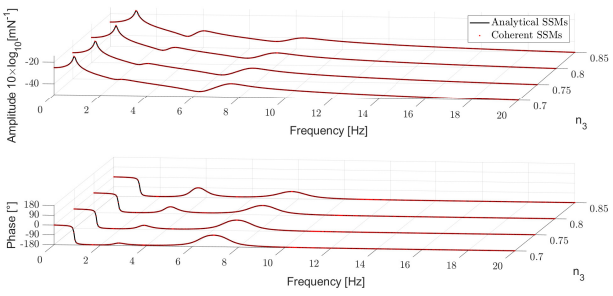

(b) Driving point displacement FRFs, whose output and input is the DOF c_1.

Figure 7: Comparison of some displacement FRFs of the set of analytical state-space models with the same displacement FRFs of their correspondent coherent representation used to set-up an LPV model representative of the dynamics of component C.

From the coherent sets of state-space models, LPV models representative of the dynamics of components A, B and C were constructed. The construction of these models was performed by parameterizing the associated time dependent variable in the multisimplex Λ of dimension $N = 2$. Moreover, each of the LPV models was assumed to present a homogeneous polynomial dependency on the correspondent time dependent variable of degree $g = 3$, because it was found that this choice leads to

the computation of LPV models with associated error vectors presenting the lowest 2-norms (see equation (29)). By solving the linear least-squares problem described in section "Linear Parameter-Varying models", the system matrices of each of the LPV models were computed. As validation, state-space models for operating fixed conditions in between the fixed conditions associated with the set of models used to define the LPV models were calculated (see table 3). Figures 8, 9 and 10 show the comparison of the FRFs of the analytical state-space models with the FRFs of the interpolated state-space models calculated by using the defined LPV models.

Table 3: Parameter values at the fixed operating conditions used to validate the LPV models

Parameter	Fixed Condition 1	Fixed Condition 2	Fixed Condition 3	Fixed Condition 4
n_1	1.025	1.075	1.115	1.135
n_2	0.875	0.915	0.935	0.97
n_3	0.715	0.735	0.775	0.825

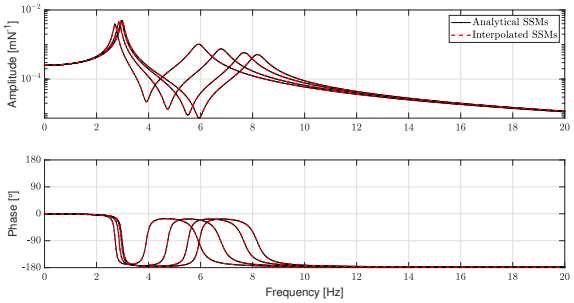

(a) Driving point displacement FRFs, whose output and input is the DOF a_1.

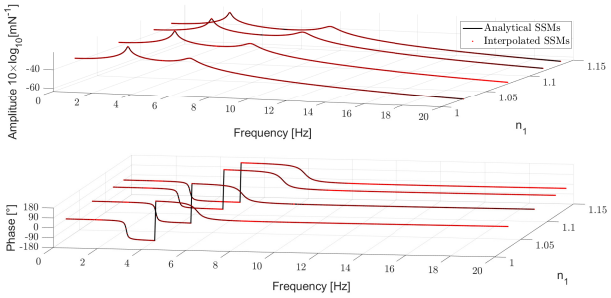

(b) Displacement FRFs, whose output is the DOF a_2 and the input is the DOF a_1.

Figure 8: Comparison of some displacement FRFs of the analytical state-space models of component A associated with the fixed conditions given in table 3 with the same FRFs of the interpolated state-space models obtained by using the computed LPV model representative of the dynamics of system A.

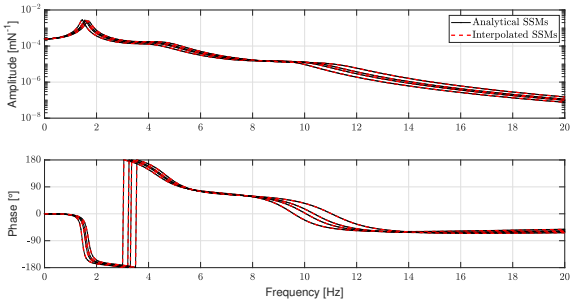

(a) Displacement FRFs, whose output is the DOF b_3 and the input is the DOF b_1.

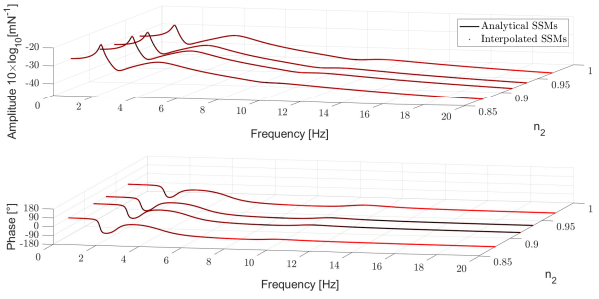

(b) Driving point displacement FRFs, whose output and input is the DOF b_2.

Figure 9: Comparison of some displacement FRFs of the analytical state-space models of component B associated with the fixed conditions given in table 3 with the same FRFs of the interpolated state-space models obtained by using the computed LPV model representative of the dynamics of system B.

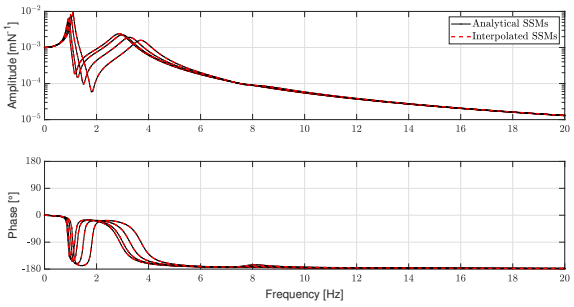

(a) Driving point displacement FRFs, whose output and input is the DOF c_3.

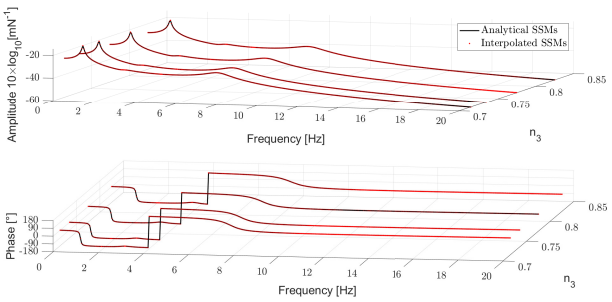

(b) Displacement FRFs, whose output is the DOF c_2 and the input is the DOF c_1.

Figure 10: Comparison of some displacement FRFs of the analytical state-space models of component C associated with the fixed conditions given in table 3 with the same FRFs of the interpolated state-space models obtained by using the computed LPV model representative of the dynamics of system C.

By observing figures 8, 9 and 10, we may conclude that the FRFs of the interpolated models obtained from the established LPV models very well-match the FRFs of the correspondents analytical state-space models. Therefore, we may claim that the constructed LPV models are reliable to represent the dynamics of components A, B and C, when submitted to fixed operating conditions characterized by a value of the time-varying parameter in $1 \leq n_1 \leq 1.15$, $0.85 \leq n_2 \leq 1$ and $0.7 \leq n_3 \leq 0.85$, respectively.

At this point, the assembly AB (see figure 2) will be studied by assuming that the component A is a source. The analysis will be performed for a time period of 4 s. It will be assumed that the source is switched on during 1 s generating a constant load of 10 N acting at DOF a_1. After this period, the source is switched off and the load acting in DOF a_1 vanishes.

To validate the state-space realization of the in-situ component-based TPA method presented in section "In-Situ Component-Based TPA", an equivalent force acting at the interface between components A and B will be determined in time-domain. Before implementing the state-space realization of the in-situ component-based TPA method, the operational response of the assembly AB must be calculated. To determine the operational responses of assembly AB, we have discretized each of the analytical state-space models representative of the dynamics of assembly AB at each time sample by using a sampling frequency of 2×10^4 Hz and the first-order-hold method (see [24]). Then, the operational responses of assembly AB, were computed by using the discretized state-space models as follows

$$\begin{aligned} \{x^{AB}(k+1)\} &= \left[A^{AB}(k)\right]\{x^{AB}(k)\} + \left[B^{AB}(k)\right]\begin{Bmatrix} u_{a_1}^{AB}(k) \\ u_J^{AB}(k) \\ u_{b_2}^{AB}(k) \\ u_{b_3}^{AB}(k) \end{Bmatrix} \\ \begin{Bmatrix} \ddot{y}_{a_1}^{AB}(k) \\ \ddot{y}_J^{AB}(k) \\ \ddot{y}_{b_2}^{AB}(k) \\ \ddot{y}_{b_3}^{AB}(k) \end{Bmatrix} &= \left[C_{accel}^{AB}(k)\right]\{x^{AB}(k)\} + \left[D_{accel}^{AB}(k)\right]\begin{Bmatrix} u_{a_1}^{AB}(k) \\ u_J^{AB}(k) \\ u_{b_2}^{AB}(k) \\ u_{b_3}^{AB}(k) \end{Bmatrix} \end{aligned} \tag{30}$$

where, k denotes the sample under analysis and superscript AB denotes variables associated with a state-space model representative of assembly AB. The same approach was exploited to compute the operational responses of assembly AC. It is worth mentioning that even though the responses computed by using expression (30) are denoted as analytical from now on, when dealing with structures presenting a non-linear mechanical behaviour, they will in fact represent linearized responses of the system. Obviously, as the used sampling frequency to discretize the state-space models is increased, better will be the match between the exact and the linearized responses.

By using the state-space realization of the in-situ component-based TPA method and the operating acceleration responses at the interface DOF and at DOFs b_2 and b_3 of assembly AB, we aim at characterizing the source by determining an equivalent

force. However, to compute the equivalent force by following this approach, acceleration state-space models representative of the assembly AB at each time sample must be available. These state-space models will be computed by exploiting two different strategies. In the first strategy, the intended state-space models will be obtained by coupling with LM-SSS the analytical displacement models (see, [25]) representative of the dynamics of systems A and B at each sample. The redundant states originated from each coupling operation will be eliminated by following the post-processing procedure presented in [26] that relies on the use of a Boolean localization matrix. In the second methodology, the coupled state-space models will be computed by coupling the displacement models of substructures A and B obtained at each sample from the interpolating LPV models. Note that, as the state-space models obtained from the interpolating LPV models are represented in the modal domain, before being coupled, they were transformed into unconstrained coupling form (UCF) (see, [25]) in order to enable the elimination of the redundant states originated from the coupling operations. Once again, the elimination of the redundant states was performed by following the post-processing procedure presented in [26] that relies on the use of a Boolean localization matrix. Both described methodologies lead to the computation of displacement coupled state-space models, hence we are required to double-differentiate them (see, [27]) in order to obtain the coupled acceleration state-space models of assembly AB required by the state-space realization of the in-situ component-based TPA method presented in section "In-Situ Component-Based TPA".

Figure 11a shows the comparison of: a) the analytical equivalent force in time-domain (see expression (6)), b) the equivalent forces estimated by using the state-space realization of the in-situ component-based TPA method with the coupled state-space models obtained at each sample from the analytical models of components A and B and c) the equivalent forces estimated by using the state-space realization of the in-situ component-based TPA method with the coupled state-space models obtained at each sample from the state-space models of components A and B computed with the defined interpolating LPV models. Figure 11b presents the comparison of: i) the reference operational acceleration response at DOF c_2 of the assembly AC, ii) the estimated operational acceleration response at the same DOF computed by using the equivalent forces obtained with approach b) and the acceleration coupled state-space models representative of assembly AC computed by coupling at each sample the analytical models of components A and C and iii) the estimated operational acceleration response at DOF c_2 of assembly AC by exploiting the equivalent force computed with methodology c) and the coupled state-space models representative of assembly AC obtained by coupling at each sample the models representative of components A and C determined from the respective LPV models.

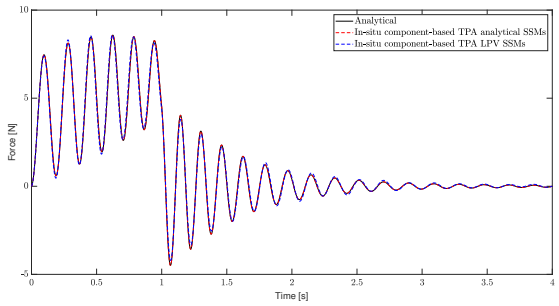

(a) Equivalent Force.

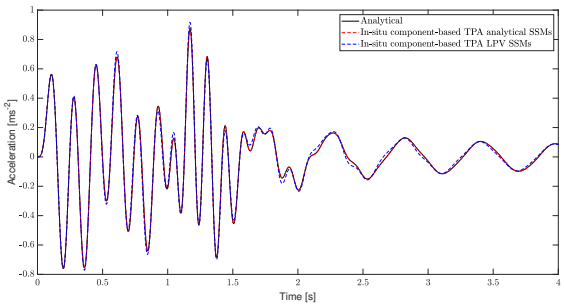

(b) Operational acceleration response of DOF c_2 of assembly AC.

Figure 11: Comparison of the computed equivalent force and of the operational acceleration response at the DOF c_2 of assembly AC by following three different methodologies.

Figure 11a suggests that the estimated equivalent force by following approach b) perfectly matches the analytical equivalent force. More importantly, the operational responses at the passive side of assembly AC (which is composed by the same source as assembly AB, but by a different passive component) estimated with this equivalent force perfectly match the analytical operational responses of this assembly. Hence, proving that the equivalent force computed by the state-space realization of the in-situ component-based TPA method is an inherent property of the source itself and, thus, transferable to structures composed by the same source linked to any other passive component.

As the equivalent force estimated with the methodology c) is concerned, we may conclude that it is well-matching the analytical equivalent force, leading to a well-matching reconstruction of the operational response at the DOF c_2 of assembly AC (see figure 11). Thus, we may claim that the joint use of the state-space realization of the in-situ component-based TPA with coupled state-space models computed by coupling models estimated from LPV models represents a reliable approach to compute equivalent forces in time-domain, when dealing with systems presenting time-varying dynamic behaviour.

To demonstrate the benefit of taking into account the time-varying dynamic behaviour of assembly AB, the equivalent force was re-computed by only using the coupled state-space model representative of AB for $n_1 = n_2 = 1$, hence by neglecting the time-variation of the dynamics of assembly AB. Figure 12a shows the comparison of this equivalent force with the analytical equivalent force and with the equivalent force obtained from methodology c). By using the equivalent force computed by assuming that the dynamics of assembly AB remain unchanged over time and by using the analytical state-space model representative of assembly AC for $n_1 = 1$ and $n_3 = 0.7$, the operating acceleration response at DOF c_2 of assembly AC was predicted. Figure 12b reports the comparison between the predicted operational response at DOF c_2 of assembly AC without taking into account the time-variation of the dynamics of both assemblies AB and AC with the reference operational acceleration response and with the same operational response computed by following approach iii),

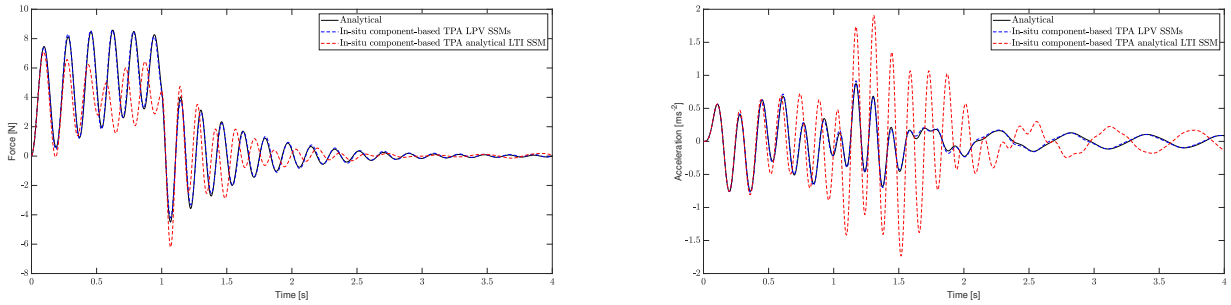

(a) (b)

Figure 12: Comparison of the computed equivalent force (figure 12a) and operational acceleration response at the DOF c_2 of assembly AC (figure 12b) by following two different methodologies that take into account the time-varying dynamical behaviour of the assemblies AB and AC with the computed equivalent force and operational acceleration response at the DOF c_2 of assembly AC by using an approach that neglects the time-varying behaviour of the assemblies AB and AC.

By observing figure 12a, it is straightforward to conclude that the computed equivalent force without taking into account the time-varying dynamical behaviour of the assembly AB is not representative of the analytical solution. Moreover, the quality of the reconstructed operational response at the DOF c_2 of assembly AC is poor (see figure 12b). The poor results are a direct consequence of neglecting the time variation of the mechanical properties of several components. Hence, we may conclude that it is worth to use interpolating LPV models to take into account the time-varying behaviour of the systems under analysis. Indeed, even though the interpolating LPV models are not capable to perfectly estimate state-space models for intermediate operating conditions, the time-varying mechanical behaviour can still be accurately described leading to good quality solutions (see figure 12). Conversely, neglecting important variations of the dynamics of the structures under analysis can lead to poor solutions as demonstrated in figure 12.

As final note, it is worth mentioning that in practice it is not common to compute equivalent forces by using operational responses collected at the interface of the source with the passive system. Nevertheless, as in this section we dealt with a numerical example, we were forced to use interface operational responses to estimate the equivalent forces by using the state-space realization of the in-situ component-based TPA method, otherwise we would be required to invert a null matrix. In an experimental scenario, this issue will in general not be faced, because state-space models estimated from experimental data do not present a diagonal feed-through matrix.

CONCLUSION

The state-space realization of the in-situ component-based TPA presented in this paper demonstrated to be valid to compute time-domain equivalent forces when dealing with structures presenting time-varying dynamic behaviour (see section "Numerical Example"). Furthermore, the use of interpolating LPV models to take into account time-variations on the dynamic properties of the systems under analysis showed to be promising, enabling good estimations of equivalent forces. Thereby, opening perspectives to apply the methodologies here described in real-case scenarios.

ACKNOWLEDGEMENTS
This project has received funding from the European Union's Framework Programme for Research and Innovation Horizon 2020 (2014-2020) under the Marie Sklodowska-Curie Grant Agreement nº 858018.

REFERENCES

[1] F. Penne. "Shaping the sound of the next-generation bmw". *In:Proceedings of the International Conference on Noise and Vibration Engineering (ISMA), Leuven, Belgium*, pages 25–39, 2004.

[2] H. van der Auweraer, P. Mas, S. Dom, A. Vecchio, K. Janssens, and P. van de Ponseele. "Transfer path analysis in the critical path of vehicle refinement: The role of fast, hybrid and operational path analysis". *SAE Technical Paper 2007-01-2352*, 2007.

[3] P. Wagner, F. Bianciardi, P. Corbeels, and A. Hülsmann. "High frequency source characterization of an e-motor using component-based TPA". *SIA NVH Comfort 2021*, 2021.

[4] Maarten V. van der Seijs, Dennis de Klerk, and Daniel J. Rixen. "General framework for transfer path analysis: History, theory and classification of techniques". *Mechanical Systems and Signal Processing*, 68-69:217–244, 2016.

[5] M. Sturm and A. Moorhouse. "Robust calculation of simultaneous multichannel blocked force signatures from measurements made in-situ using an adaptive algorithm in time domain". *In: Proceedings of the 20th International Congress on Sound and Vibration (ICSV), Bangkok, Thailand*, 2:1610–1617, 2013.

[6] M. S. Allen and T. G. Carne. "Delayed, multi-step inverse structural filter for robust force identification". *Mechanical Systems and Signal Processing*, 22(5):1036–1054, 2008.

[7] Y. M. Mao, X. L. Guo, and Y. Zhao. "A state space force identification method based on markov parameters precise computation and regularization technique". *Journal of Sound and Vibration*, 329:3008–3019, 2010.

[8] M. Haeussler, S.W.B. Klaassen, and D.J. Rixen. "Experimental twelve degree of freedom rubber isolator models for use in substructuring assemblies". *Journal of Sound and Vibration*, 474:115253, 2020.

[9] J. De Caigny, J.F. Camino, and J. Swevers. "Interpolating model identification for siso linear parameter-varying systems". *Mechanical Systems and Signal Processing*, 23:2395–2417, 2009.

[10] J. De Caigny, J.F. Camino, and J. Swevers. "Interpolation-Based Modeling of MIMO LPV Systems". *IEEE Transactions on Control Systems Technology*, 19(1):46–63, 2011.

[11] J. De Caigny, R. Pintelon, J.F. Camino, and J. Swevers. "Interpolated Modeling of LPV Systems". *IEEE Transactions on Control Systems Technology*, 22(6):2232–2246, 2014.

[12] A. Steltzner and D. Kammer. "Input force estimation using an inverse structural filter". *In:* 17th *International Modal Analysis Conference, Kissimmee, Florida, USA*, pages 954–960, 1999.

[13] S. Vettori, E. Di Lorenzo, B. Peeters, M. M. Luczak, and E. Chatzi. "An adaptive-noise augmented kalman filter approach for input-state estimation in structural dynamics". *Mechanical Systems and Signal Processing*, 184, 2023.

[14] Jesús Ortega Almirón, Fabio Bianciardi, Patrick Corbeels, Rupert Ullmann, and Wim Desmet. "Mount characterization analysis in the context of fbs for component-based tpa on a wiper system". *Forum Acusticum 2020, Lyon, France*, 2020.

[15] A.S. Elliott and A.T. Moorhouse. "Characterisation of structure borne sound sources from measurement in-situ". *Journal of the Acoustical Society of America*, 123:3176–3176, 2008.

[16] A.T. Moorhouse, A.S. Elliott, and T.A. Evans. "In situ measurement of the blocked force of structure-borne sound sources". *Mechanical Systems and Signal Processing*, 325:679–685, 2009.

[17] T. McKelvey, H. Akcay, and L. Ljung. "Subspace-based multivariable system identification from frequency response data". *IEEE Transactions on Automatic Control*, 41:960–979, 1996.

[18] L. Ljung. *System Identification Theory for the User*. 2nd Edition, Prentice Hall, Upper Saddle River, NJ, 1999.

[19] Mahmoud El-Kafafy and Bart Peeters. "A Robust Identification of Stable MIMO Modal State Space Models". *In: Dilworth, B.J., Marinone, T., Mains, M. (eds) Topics in Modal Analysis & Parameter Identification, Volume 8. Conference Proceedings of the Society for Experimental Mechanics Series. Springer, Cham*, pages 81–95, 2023.

[20] R.S.O. Dias, M. Martarelli, and P. Chiariotti. "State-space domain virtual point transformation for state-space identification in dynamic substructuring". *In: Proceedings of ISMA 2022 - International Conference on Noise and Vibration Engineering and USD 2022 - International Conference on Uncertainty in Structural Dynamics*, 2022.

[21] Bart Peeters, Herman Van der Auweraer, Patrick Guillaume, and Jan Leuridan. "The polymax frequency-domain method: a new standard for modal parameter estimation?". *Schock and Vibration*, 11:395–409, 2004.

[22] Mahmoud El-Kafafy, Bart Peeters, Patrick Guillaume, and Tim De Troyer. "Constrained maximum likelihood modal parameter identification applied to structural dynamics". *Mechanical Systems and Signal Processing*, 72-73:567–589, 2016.

[23] J.H. Yung. *Gain scheduling for geometrically nonlinear flexible space structures (PhD dissertation)*. Massachusetts Institute of Technology, Cambridge, MA, USA, 2002.

[24] G. F. Franklin, D. J. Powell, and M. L. Workman. *Digital Control of Dynamic Systems*. Prentice Hall, 3^{rd} edition edition, 1997.

[25] R.S.O. Dias, M. Martarelli, and P. Chiariotti. "On the use of lagrange multiplier state-space substructuring in dynamic substructuring analysis". *Mechanical Systems and Signal Processing*, 180, 2022.

[26] R.S.O. Dias, M. Martarelli, and P. Chiariotti. "Lagrange Multiplier State-Space Substructuring". *Journal of Physics: Conference Series*, 2041(1):012016, 2021.

[27] F. Lembregts, J.Leuridan, and H. Van Brussel. "Frequency domain direct parameter identification for modal analysis: State space formulation". *Mechanical Systems and Signal Processing*, 4:65–75, 1990.